This article has been accepted for publication in a future issue of this journal, but has not been fully edited. Content may change prior to final publication.

A Novel and Fundamental Approach towards Field and Damper Circuit Parameter Determination of Synchronous Machine

Kaushik Mukherjee
Member, IEEE
University of Windsor
kmukh@uwindsor.ca

Lakshmi Varaha Iyer
Student Member, IEEE
University of Windsor
iyerl@uwindsor.ca

Xiaomin Lu
Student Member, IEEE
University of Windsor
lu117@uwindsor.ca

Narayan C. Kar
Senior Member, IEEE
University of Windsor
nkar@uwindsor.ca

Abstract **- In this era of advanced computing where complex algorithms and expensive approaches are used to determine the machine parameters of a synchronous machine, this paper proposes a novel, economical and yet fundamental approach towards estimation of the d- and q-axis field and damper circuit parameters of a low/medium power wound-field synchronous machine. The proposed novel methodology employs fundamental voltage, current, flux linkage relationships of the 3-phase wound-field synchronous machine in a-b-c reference frame theory. Firstly, the proposed methodology has been explained in detail using analytical equations and then employed to determine the aforementioned parameters of a small laboratory synchronous machine. Other equivalent circuit parameters have been determined using conventional tests. Further validation of the proposed methodology was performed using two other larger machines with different nameplate ratings. Moreover, the aforementioned parameters of the larger machines were also experimentally determined using IEEE standard tests. Finally, a comparison of the results obtained employing the conventional and the proposed methodologies were performed and the proposed methodology has been established to be valid as the results are in close agreement.**

Index Terms **- Damper circuit, field circuit, parameter estimation, wound-field synchronous machine.**

I. INTRODUCTION

Many papers have been written since the first ones by Park [1], [2] till today about the definition, characterization and measurement of electrical parameters of synchronous machines [3], [4]. Industrial test and measurement standards by world-renowned North American and European bodies viz. IEEE 115, IEEE 1110, IEC and NEMA MG1-2006 also exist for determination of parameters and stability and dynamic studies [5]-[7]. Although research on parameter determination of wound-field synchronous machines started many decades ago, this topic keeps on receiving active investigation as the need for development of fundamental, less expensive, flexible and yet reliable parameter determination procedures still exist. Knowledge of correct synchronous machine (SM) equivalent circuit parameters permits accurate predictions on power system dynamics, stability studies and real-time input power and exciter control [5]-[8], where the machine acts predominantly in the generator mode. These studies are equally important for similar dynamic studies of large high-power load commutated inverter (LCI) fed synchronous machine drives, where the machine predominantly works in the motoring mode [9] in applications such as pumped storage and ship propulsion. Accurate parameters for dynamic studies for predicting and analyzing changeover of modes with perspective to success of load/induced voltage commutation of the LCI drive thyristors at all loads and transient overvoltage during load commutation across the thyristors are of paramount importance [10]. Small and medium power wound field synchronous machine for drives applications also require parameter information obtained through simple yet reasonably accurate means for high performance parameter-sensitive real-time drive control applications [11]. Studies conducted in the early 1970s [12] showed that, in general, in stability analysis it is more important to use accurate machine data than to use more elaborate machine models. In developing and applying more detailed and accurate models [13], [14], it was found that an economic benefit could be obtained from the increased capability to transmit power generated at a lower cost site. Background literature obtained from [5]-[14] state that the standard tests used to determine the SM parameters are the short-circuit tests, standstill frequency response (SSFR) and time domain tests.

Owing to their simplicity of implementation, off-line tests such as standstill frequency response (SSFR) and standstill time domain (SSTD) tests, have attracted the attention of researchers [15]-[19]. One noteworthy advantage about why SSFR testing has become an acceptable alternative to short-circuit testing is that identification of field winding response is possible. They pose a low probability of risk to the machine being tested, and data in both direct and quadrature axes are available, with little change in the test setup without resorting to special short circuit and/or low-voltage tests.

Copyright (c) 2013 IEEE. Personal use is permitted. For any other purposes, permission must be obtained from the IEEE by emailing pubs-permissions@ieee.org.

This article has been accepted for publication in a future issue of this journal, but has not been fully edited. Content may change prior to final publication.

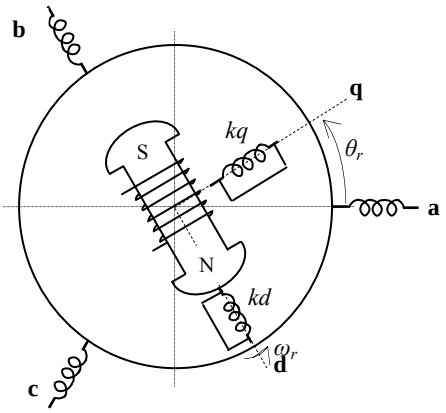

Fig. 1. Winding schematics of a 3-phase wound field synchronous machine demonstrating the winding dispositions, electrical rotor position and the d-q rotor reference frame.

However, the inaccuracy of the results obtained from the SSFR test due to the required nonstandard condition of machine operation still exists. For this reason, the analysis of SSFR test data usually yields models requiring further adjustments to correct for the overly low magnetizing currents that tend to occur during test. Hence, the data obtained from SSFR test is adjusted by data obtained by complementary short circuit tests or the online frequency response tests. Otherwise, the SSFR test requires supplementary tests to be performed along with it in order to provide accurate results, thus, making it complex and time consuming.

Even though the authors reiterate that the SSFR test is a well established process that allows the determination of high-order models on synchronous machines, sophisticated equipment, such as a function generator, a large fundamental frequency AC power source (power converter/amplifier) and a spectrum analyzer, are required. Also the SSFR test is found to be time consuming at lower frequency range of 0.001– 0.01 Hz [20]. Problem noise, probably due to winding heating, in the lower frequency range is a disadvantage of the SSFR test.

Moreover, keeping in view the educational sector, where the synchronous machine is taught as one of the fundamental machines along with the induction and the DC machines, laboratory experiments are usually performed on fractional horsepower machines which do not always obey the IEEE standards of parameter estimation [5]. Also, if experiments are performed on bigger machines, specialized equipment involved such as the function generator, power amplifier and spectrum analyzer might have to be purchased to perform the SSFR tests and cost of obtaining technical specialists would be another issue.

Hence, this research manuscript proposes a novel and yet fundamental approach towards determining the field circuit and d- and q-axis damper circuit resistances and inductances, by employing basic voltage, current, flux linkage relationships of the 3-phase wound field synchronous machine in a-b-c reference frame theory. This proposed methodology rests on the assumption of the presence of one d-axis damper and one q-axis damper winding in the machine and hence is predicted towards use with small or medium sized hydro-alternators or synchronous motors meant for low/medium power machine drives applications. Section II explains in length the derivation of the analytical model of the proposed methodology for parameter estimation. Experiments have been performed on a 120 VA machine, a 1.5 kVA machine and a 5 kVA machine based on the proposed method and results are investigated and validated in section III and IV respectively. Supporting data of other machine parameters such as the armature resistance, armature leakage reactance, d- and q-axis magnetizing reactances, have been obtained through conventional tests [5].

II. The Proposed Methodology and Its Derivation to Determine Field and Damper Circuit Parameters

The voltage equation of phase 'a' (Fig. 1) of a three phase wound field synchronous machine is given by:

$$v_{an} = r_a i_a + p\psi_a \tag{1}$$

where, v_{an}, i_a are the armature 'a' phase voltage and current respectively, r_a is the armature phase resistance, ψ_a is the total flux linkage of the a-n winding and p is the differential *(d/dt)* operator. For a general three-phase salient-pole synchronous machine with one d-axis damper and one q-axis damper, the time rate of change of the flux linkage of the 'a' phase armature winding can be written as [21]:

$$\begin{aligned} p\psi_a = p[&\{L_{la} + L_A - L_B\cos 2\theta_r\}i_a \\ &+ \{-0.5L_A - L_B\cos(2\theta_r - 2\pi/3)\}i_b \\ &+ \{-0.5L_A - L_B\cos(2\theta_r + 2\pi/3)\}i_c \\ &+ L_{mq}\cos\theta_r i'_{kq} + L_{md}\sin\theta_r i'_{fd} + L_{md}\sin\theta_r i'_{kd}] \end{aligned} \tag{2}$$

where, L_{la} is the armature leakage inductance, L_{md} and L_{mq} are the d-axis and q-axis magnetizing inductances, i_b, i_c are the currents of the other two armature phases, θ_r is the rotor position (electrical) as shown in Fig. 1, i'_{kq}, i'_{fd} and i'_{kd} are the currents in the q-axis damper, field and d-axis damper windings respectively, referred to armature, L_A and L_B are inductances related to L_{md} and L_{mq} by the following expressions:

$$L_{md} = \frac{3}{2}\left(L_A + L_B\right) \tag{3}$$

$$L_{mq} = \frac{3}{2}\left(L_A - L_B\right) \tag{4}$$

Motoring condition has been assumed positive here. In the proposed methodology for determining the electrical parameters of the field and dampers of the conventional d-axis and q-axis equivalent circuit, only a controlled single phase AC sinusoidal voltage would be applied to the armature a-phase winding with the rotor held stationary at certain strategic stationary positions. With the rotor at stationary position, $p\theta_r = \omega_r = 0$, where, ω_r is the rotor speed in electrical radian per second. Hence,

Copyright (c) 2013 IEEE. Personal use is permitted. For any other purposes, permission must be obtained from the IEEE by emailing pubs-permissions@ieee.org.

This article has been accepted for publication in a future issue of this journal, but has not been fully edited. Content may change prior to final publication.

$$\begin{aligned} p\psi_a &= (pi_a)(L_{la} + L_A - L_B\cos 2\theta_r) \\ &+ (pi_b)\{-0.5L_A - L_B\cos(2\theta_r - 2\pi/3)\} \\ &+ (pi_c)\{-0.5L_A - L_B\cos(2\theta_r + 2\pi/3)\} \\ &+ L_{mq}\cos\theta_r(pi'_{kq}) + L_{md}\sin\theta_r(pi'_{kd}) + L_{md}\sin\theta_r(pi'_{fd}) \end{aligned} \quad (5)$$

Under an operating condition, when a-phase is aligned with d-axis (i.e. field axis), kept stationary and is excited with a single phase sinusoidal AC voltage with the other two phases kept open (i.e. $\theta_r = 90^0$, i_b=i_c=0, $pi_b = pi_c = 0$),

$$p\psi_a = (pi_a)(L_{la} + L_A + L_B) + L_{md}(pi'_{fd}) + L_{md}(pi'_{kd}) \quad (6a)$$

$$p\psi_a = (pi_a)(L_{la} + \tfrac{2}{3}L_{md}) + L_{md}(pi'_{fd}) + L_{md}(pi'_{kd}) \quad (6b)$$

$$p\psi_a = \tfrac{2}{3}(pi_a)(\tfrac{3}{2}L_{la} + L_{md}) + L_{md}(pi'_{fd}) + L_{md}(pi'_{kd}) \quad (6c)$$

Therefore,

$$\begin{aligned} v_{an} &= [(2/3)i_a(3/2)r_a + (2/3)(pi_a)\{(3/2)L_{la} + L_{md}\} \\ &+ L_{md}(pi'_{fd}) + L_{md}(pi'_{kd})] \end{aligned} \quad (7)$$

v'_{fd}, the terminal voltage of the field winding, referred to armature, can be written as:

$$\begin{aligned} v'_{fd} &= (\tfrac{2}{3})L_{md}\,p(i_a\sin\theta_r) + (\tfrac{2}{3})L_{md}\,p(i_b\sin(\theta_r - 2\pi/3)) \\ &+ (\tfrac{2}{3})L_{md}\,p(i_c\sin(\theta_r + 2\pi/3)) + i'_{fd}r'_{fd} \\ &+ (L_{md} + L'_{lf})(pi'_{fd}) + L_{md}(pi'_{kd}) \end{aligned} \quad (8a)$$

where, r'_{fd} is the field winding resistance referred to armature, L'_{lf} is the leakage inductance of the field referred to armature. Under the same operating conditions corresponding to (6a),

$$\begin{aligned} v'_{fd} &= (\tfrac{2}{3})L_{md}\sin\theta_r(pi_a) + (\tfrac{2}{3})L_{md}(\sin(\theta_r - 2\pi/3))(pi_b) \\ &+ (\tfrac{2}{3})L_{md}(\sin(\theta_r + 2\pi/3))(pi_c) + i'_{fd}r'_{fd} \\ &+ (L_{md} + L'_{lf})(pi'_{fd}) + L_{md}(pi'_{kd}) \end{aligned} \quad (8b)$$

$$v'_{fd} = [i'_{fd}r'_{fd} + (\tfrac{2}{3})L_{md}(pi_a) + (L_{md} + L'_{lf})(pi'_{fd}) + L_{md}(pi'_{kd})] \quad (8c)$$

The Kirchoff's voltage law in the short-circuited d-axis damper winding can be written as:

$$\begin{aligned} 0 = v'_{kd} &= (\tfrac{2}{3})p[i_aL_{md}\sin\theta_r + i_bL_{md}\sin(\theta_r - 2\pi/3) \\ &+ i_cL_{md}\sin(\theta_r + 2\pi/3)] + i'_{kd}r'_{kd} \\ &+ p[L_{md}i'_{fd} + (L'_{lkd} + L_{md})i'_{kd}] \end{aligned} \quad (9a)$$

where, L'_{lkd} is the d-axis damper leakage inductance referred to armature. Under the same operating condition mentioned earlier,

$$\begin{aligned} 0 = v'_{kd} &= (\tfrac{2}{3})L_{md}(pi_a) + i'_{kd}r'_{kd} + L_{md}(pi'_{fd}) \\ &+ (L'_{lkd} + L_{md})pi'_{kd} \end{aligned} \quad (9b)$$

$$0 = v'_{kd} = [L_{md}\,p((\tfrac{2}{3})i_a + i'_{fd} + i'_{kd}) + i'_{kd}r'_{kd} + L'_{lkd}(pi'_{kd})] \quad (9c)$$

As the d-axis is kept aligned with armature 'a' phase at stationary condition, armature phases 'b', 'c' and the field kept open and a controlled single phase AC voltage (v_{an}) applied across the armature 'a' phase, with the actual current i_a flowing in the same phase, (7), (8c) and (9c) under this operating condition gives rise to the electrical equivalent circuit of Fig. 2, where a conceptual current of $0.67i_a$ flows in

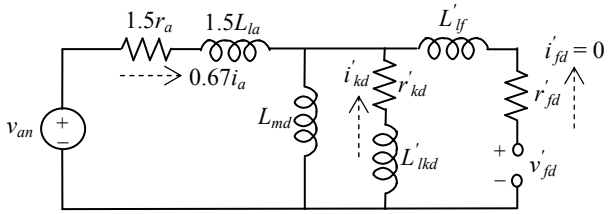

Fig. 2. Equivalent electrical circuit under operating condition #1, when a single phase sinusoidal voltage has been applied across 'a' phase winding, with 'a' phase kept aligned with d-axis and other phases and field winding kept open.

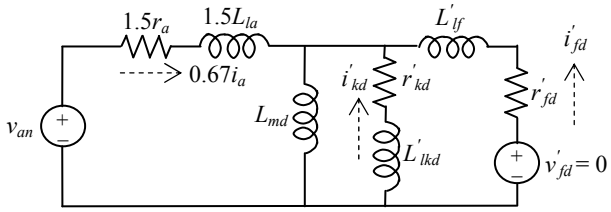

Fig. 3. Equivalent electrical circuit under operating condition #2, when a single phase sinusoidal voltage has been applied across 'a' phase winding, with 'a' phase kept aligned with d-axis, other phases kept open and field winding kept shorted.

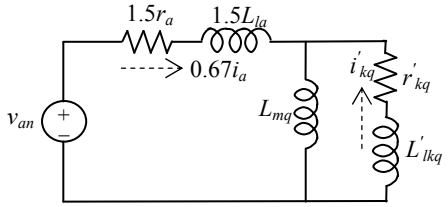

Fig. 4. Equivalent electrical circuit under operating condition #3, when a single phase sinusoidal voltage has been applied across 'a' phase winding, with 'a' phase kept aligned with q-axis, other phases and field winding kept open.

the armature side. This is operating condition #1. Operating condition #2 prevails when the field winding is kept shorted with all other settings of operating condition #1 kept same. Equations (7), (8c) and (9c) under this condition give rise to the equivalent circuit of Fig. 3. Under operating conditions similar to that of #1, but now with q-axis aligned with the a-phase axis at stationary position (θ_r= 0^o), designated as operating condition #3, the Kirchoff's voltage law in the a-phase of the armature and the q-axis damper can be similarly derived as:

$$v_{an} = (\tfrac{2}{3})i_a(\tfrac{3}{2}r_a) + (\tfrac{2}{3})(pi_a)[(\tfrac{3}{2})L_{la} + L_{mq}] + L_{mq}(pi'_{kq}) \quad (10)$$

$$0 = v'_{kq} = [L_{mq}\,p((\tfrac{2}{3})i_a + i'_{kq}) + i'_{kq}r'_{kq} + L'_{lkq}(pi'_{kq})] \quad (11)$$

where, L'_{lkq} is the q-axis damper leakage inductance referred to armature. With the help of equations (10) and (11), the equivalent electrical circuit of Fig. 4 can be formulated for operating condition #3. With the knowledge of r_a, L_{la}, L_{md} and L_{mq}, the field and damper parameters of the conventional d-axis and q-axis equivalent circuits can be easily obtained by

Copyright (c) 2013 IEEE. Personal use is permitted. For any other purposes, permission must be obtained from the IEEE by emailing pubs-permissions@ieee.org.

This article has been accepted for publication in a future issue of this journal, but has not been fully edited. Content may change prior to final publication.

solving the equivalent circuits of Figs. 2, 3 and 4 under the three operating conditions if experiments are performed accordingly. Here lies the novelty of this paper and to the best knowledge of the authors, such an approach for finding out the field and the damper parameters has not been proposed or employed until date.

III. Experimental Results Employing the Proposed Methodology

Experiments have been performed on three 3-phase wound field synchronous machines of three different ratings to establish the universality of the proposed methodology and technique for low and medium power synchronous machines. The ratings of all the machines used have been furnished in the Appendix. The armature DC resistance is experimentally found out by performing DC drop tests and r_a is considered 20% more to account for AC resistance effects [22]. The armature leakage inductance (L_{la}) is experimentally obtained from the Potier reactance obtained jointly from open-circuit characteristics (O.C.C.), short circuit characteristics (S.C.C.), and zero power factor characteristics test (ZPF) performed at rated voltage [5], [23]. The leakage inductance value is ultimately obtained from the Potier reactance by considering a factor as outlined in [23]. It is to be mentioned here that complex effects of saturation have not been taken into account here as the main focus of this paper is towards establishing the novel methodology of finding the equivalent circuit field and damper parameters by formulating three special simple machine equivalent circuits.

The d-axis synchronous inductance (L_d) is found out by conducting O.C.C and S.C.C tests [5] and L_{md} has been obtained as the difference of L_d and L_{la}. Slip test has been performed to obtain the ratio of d-axis synchronous inductance to the q-axis synchronous inductance [5] and hence L_{md}/L_{mq} ratio is derived. With the knowledge of L_{md} already obtained, L_{mq} value is found out.

TABLE I
Parameters from Established Test Methods For the 3 Machines

Parameter	Tests performed	Value determined	Comments
r_a	DC drop test	Machine #1 - 12.31 Ω Machine #2 – 5.8 Ω Machine #3 – 0.6 Ω	The final value is taken 20% more than the DC resistance to account for AC resistance
L_{la}	Open circuit test, short circuit test, zero power factor test at rated speed (Potier reactance)	Machine #1 - 59.68 mH Machine #2 – 17 mH Machine #3 – 3.662 mH	The value is fine-tuned as per [23] to have a true essence of the armature leakage reactance from Potier reactance test.
L_{md}	Open circuit test, short circuit test at rated speed	Machine #1 - 350 mH Machine #2 – 83 mH Machine #3 – 70.22 mH	As per IEEE standard [5]
L_{mq}	Slip test, Maximum lagging current test	Machine #1 - 343 mH Machine #2 – 47 mH Machine #3 – 61.24 mH	As per IEEE standard [5] and [24].

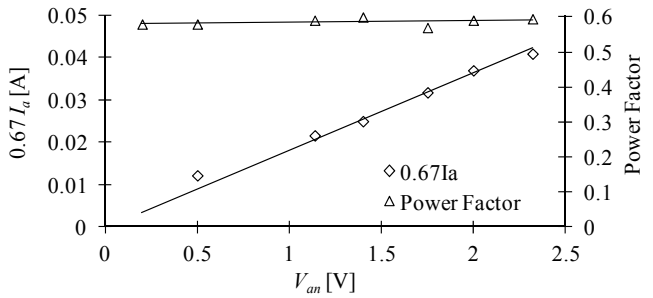

Fig. 5. Experimental observations of input current ($0.67I_a$) and input power factor versus applied input voltage (V_{an}) of the equivalent circuit of Fig. 2 under operating condition #1 for Machine #1.

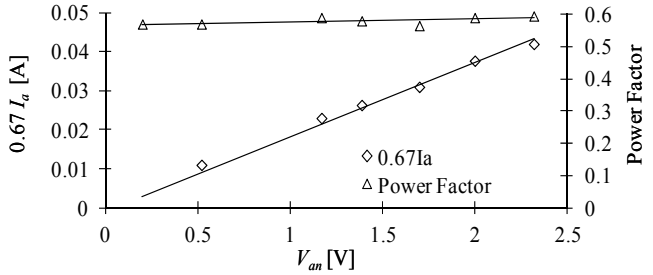

Fig. 6. Experimental observations of input current ($0.67I_a$) and input power factor versus applied input voltage (V_{an}) of the equivalent circuit of Fig. 3 under operating condition #2 for Machine #1.

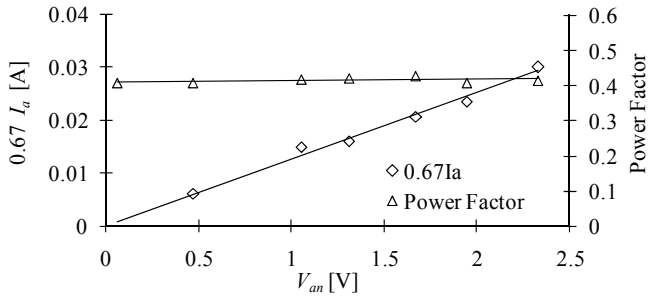

Fig. 7. Experimental observations of input current ($0.67I_a$) and input power factor versus applied input voltage (V_{an}) of the equivalent circuit of Fig. 4 under operating condition #3 for Machine #1.

The value of L_{mq} is further cross-checked from the maximum lagging current test which is considered more accurate [5], [24], [25].

The aforementioned tests, following established references, yield accurate values of r_a, L_{la}, L_{md} and L_{mq} and the experimental results are furnished in Table I for the three tested machines. Knowledge about these parameters now set the tone for determining the field and damper parameters experimentally with the help of the three equivalent circuits of Figs. 2, 3 and 4 for three different operating conditions, explained earlier. These conditions are next achieved through experiments. The alignment of 'a' phase with the d-axis has been performed by exciting the field winding and the a-phase winding with controlled DC current with proper polarities, which produce enough torque to rotate and get aligned or locked. The alignment of 'a' phase with q-axis is achieved by

Copyright (c) 2013 IEEE. Personal use is permitted. For any other purposes, permission must be obtained from the IEEE by emailing pubs-permissions@ieee.org.

This article has been accepted for publication in a future issue of this journal, but has not been fully edited. Content may change prior to final publication.

exciting the field winding, 'b' and 'c' phases with proper polarities. After a particular alignment is over (operating conditions #1 and #2 for d-axis alignment and #3 for q-axis alignment), DC supplies are removed and for each operating condition, a single phase variac controlled power frequency (60 Hz) AC voltage is impressed on the armature 'a' phase (v_{an}). Current i_a and the input power factor (PF) are noted for each voltage under each operating condition (#1, #2 and #3).

The input impedance of the equivalent circuits of Figs. 2, 3 and 4 ($V_{in}/0.67I_a$) and the input power factors, experimentally obtained for different values of applied voltages in each operating condition, are presented in Figs. 5, 6 and 7 respectively for Machine #1. Typical oscilloscopic waveforms of v_{an} and i_a at steady state for operating condition#1, #2 and #3 are furnished in Figs. 8, 9 and 10 respectively for the same machine, where from the power factors at the respective operating conditions are evident. Investigation of the equivalent circuit of Fig. 2 reveals that in operating condition #1 with the field open, with r_a, L_{la}, L_{md} known, the two unknowns r'_{kd} and L'_{lkd} can be found out from the knowledge of the input impedance value and input power factor (Fig. 5) of the same circuit. The obtained average values have been presented in Table II.

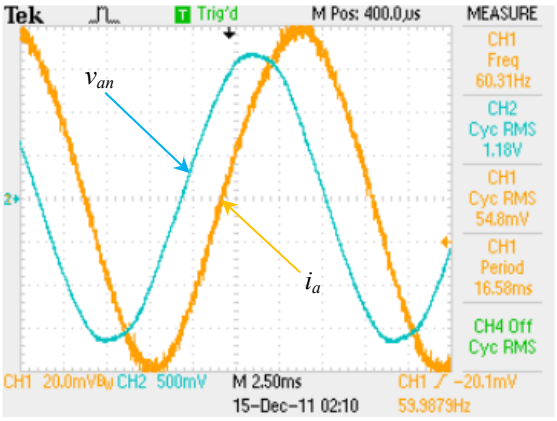

Fig. 8. Experimental v_{an} and i_a waveforms under operating condition #1 with armature 'a' phase aligned with d-axis with field winding kept open for Machine #1.

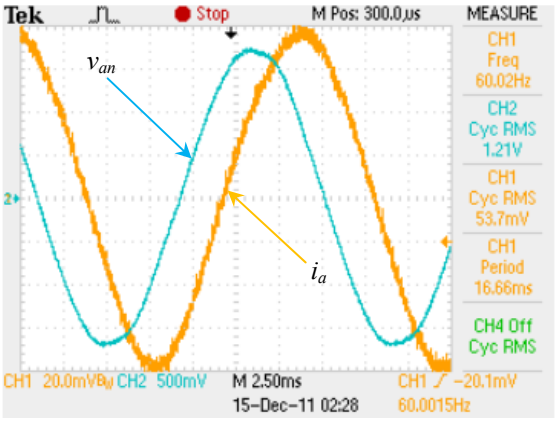

Fig. 9. Experimental v_{an} and i_a waveforms under operating condition #2 with armature 'a' phase aligned with d-axis with field winding kept shorted for Machine #1.

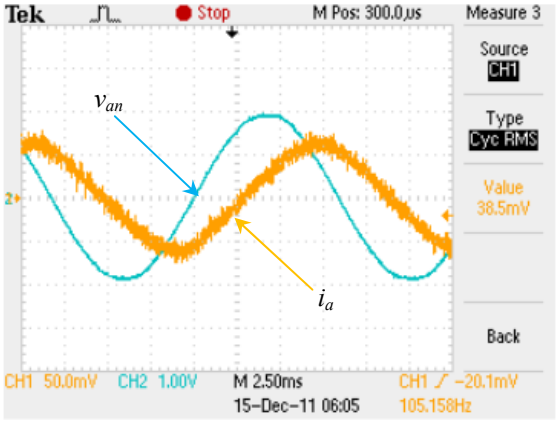

Fig. 10. Experimental v_{an} and i_a waveforms under operating condition #3 with armature 'a' phase aligned with q-axis with field winding kept open for Machine #1.

TABLE II
PARAMETERS OBTAINED FROM PROPOSED TEST METHOD

Parameter	Value determined for Machine #1	Value determined for Machine #2	Value determined for Machine #3
r'_{fd}	142.83 Ω	0.31 Ω	0.14 Ω
L'_{lf}	145.4 mH	9.2 mH	12.4 mH
r'_{kd}	16.24 Ω	16 Ω	0.827 Ω
L'_{lkd}	25.18 mH	60 mH	4.677 mH
r'_{kq}	32.67 Ω	4 Ω	2.11 Ω
L'_{lkq}	139 mH	51 mH	11.11 mH

With r'_{kd} and L'_{lkd} thus found out, for operating condition #2 with field shorted, examination of the equivalent circuit of Fig. 3 shows that there are two unknowns, r'_{fd} and L'_{lf}. These have been experimentally obtained from the knowledge of input impedance and power factor (Fig. 6) of the circuit of Fig. 3 and the average values are given in Table II.

The q-axis damper parameters r'_{kq} and L'_{lkq} have been found out similarly as r'_{kd} and L'_{lkd} by solving the equivalent circuit of Fig. 3 from the impedance and power factor obtained from Fig. 7. The mean values are finally entered in Table II. Similar exercises have been performed on Machine #2 and #3 and the results are presented in the same table. If the resistance of the field winding (r_f) is experimentally obtained by DC drop test, the r'_{fd} / r_f ratio of the machine would yield the N_f / N_a turns ratio of the equivalent sinusoidally distributed armature winding and field winding and correlation between actual parameters and referred parameters can be performed very easily. This would be particularly relevant for steady state and dynamic analyses of synchronous machines in general.

The procedure for obtaining the field and damper circuit parameters can therefore be summarized as follows:

Step 1: Perform the equivalent circuit parameters r_a (armature resistance), L_{la} (armature leakage inductance), L_{md} (d-axis magnetizing inductance) and L_{mq} (q-axis magnetizing inductance) from any standard test, as applicable [5].

Step 2: Align armature 'a'-phase with d-axis and keep rotor stationary. Once aligned and kept stationary, it will not have any tendency to rotate by itself due to the subsequent steps as no torque will be produced. Excite a single phase sinusoidal

Copyright (c) 2013 IEEE. Personal use is permitted. For any other purposes, permission must be obtained from the IEEE by emailing pubs-permissions@ieee.org.

This article has been accepted for publication in a future issue of this journal, but has not been fully edited. Content may change prior to final publication.

AC voltage to 'a'-phase with the other two phases and field winding kept open. Measure 'a'-phase applied voltage (v_{an}), resultant 'a'-phase current (i_a) and corresponding input power factor, equivalent electrical circuit shown in Fig. 2 (It is to be noted that the input current in Fig. 2 should be treated as $0.67i_a$ if the actual current obtained experimentally is i_a). The set of measurement for machine I is shown in Fig. 5. Obtain damper d-axis current i'_{kd} (magnitude and phase) using (7), considering $i'_{fd} = pi'_{fd} = 0$. Based on determined i'_{kd}, calculate damper d-axis parameters r'_{kd} and L'_{lkd} by solving with corresponding equations (9c).

Step 3: Align 'a'-phase with d-axis and keep rotor stationary. Excite a single phase sinusoidal AC voltage to 'a'-phase with the other two phases kept open and field kept shorted, equivalent electrical circuit shown in Fig. 3. Measure 'a'-phase applied voltage (v_{an}), resultant 'a'-phase current (i_a) and corresponding input power factor, equivalent electrical circuit shown in Fig. 3 (It is to be noted that the input current in Fig. 2 should be treated as $0.67i_a$ if the actual current obtained experimentally is i_a). The set of measurement for machine I is shown in Fig. 6. Obtain field short circuit current, i'_{fd} using (7) and 9(c). Based on determined i'_{fd}, with d-axis damper parameters already found out, calculate field parameters r'_{fd} and L'_{fd} by solving equivalent electrical circuit in Fig. 3 with corresponding equations 8(b).

Step 4: Next, align a-phase with q-axis and keep rotor stationary. Excite a single phase sinusoidal AC voltage to a-phase with the other two phases and field open, equivalent electrical circuit shown in Fig. 4. Measure 'a'-phase applied voltage (v_{an}), resultant 'a'-phase current (i_a) and corresponding input power factor, in a way similar to step 2 or 3 above. The set of measurement for machine I is shown in Fig. 7. Obtain damper q-axis current i'_{kq} (magnitude and phase) using (10). Based on determined i'_{kq}, calculate damper q-axis parameters r'_{kq} and L'_{lkq} by solving with corresponding equations (11).

IV. Experimental Validation of the Proposed Methodology

The proposed methodology is verified by two ways on Machine #2 and #3 by comparing the results obtained from them as per the proposed test technique against those determined from experiments employing existing/reported methodologies in the literatures.

First method of validation:

It is already reported that the rate of rise/fall of current in a particular armature phase and the spike generated in the corresponding terminal (phase) voltage during commutation of the thyristors in a '120^0 conduction LCI drive' are heavily dependent on the synchronous machine's subtransient and transient reactances and time constants, which are functions of the field and damper parameters [26, 27]. Hence, machine #2 is as motor by a load-commutated inverter (LCI) by keeping the field winding in the DC link yielding series characteristics in a similar way as in [26]. The block diagram of the experimental setup is presented in Fig. 11. Figs. 12 (a) and (b) show the experimental waveforms of one armature

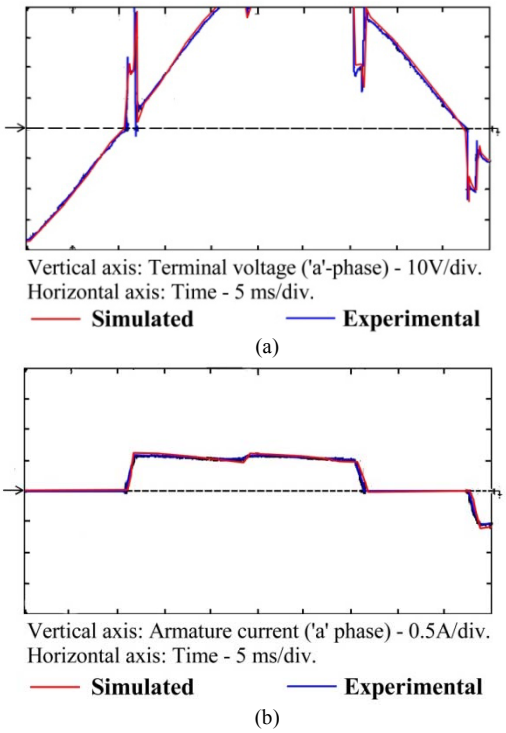

Fig. 12. Experimental and simulated waveforms (commutating intervals of thyristors zoomed in) of the 120 degree conduction LCI-fed synchronous motor drive with Machine #2 of Fig. 11. (a) Armature terminal voltage of 'a' phase. (b) Armature current of 'a' phase.

phase (terminal) voltage waveform and the corresponding phase current waveform respectively of the LCI drive of Fig. 11 under a particular steady state loading. A detailed numerical model is developed to simulate the same LCI drive including 120^0 conduction of the thyristors, employing the electrical parameters of the same machine, as obtained experimentally by following the proposed methodology, presented in Table II. The terminal (phase) voltage and the phase current waveforms, as predicted by this numerical model, are presented in Figs. 12 (a) and (b) along with the respective experimental waveforms under identical operating conditions. These simulated waveforms, basis of which are the electrical parameters obtained from experiments as per the proposed methodology, would not have been so close to the experimental waveforms of the actual LCI drive employing machine #2, had the proposed methodology been wrong. The closeness of these experimental and simulated waveforms, furnished in Figs. 12 (a) and (b), thus clearly validates the proposed methodology of determining the field and damper parameters.

Second method of validation:

An established method of determining a synchronous machine's d-axis transient and subtransient reactances and time constants, which are functions of the armature, field and the damper parameters, is from oscillogram of the armature currents, when the machine is exposed to a symmetrical short circuit with an armature voltage much less than the rated, before the short circuit [5]. The q-axis subtransient reactance is conventionally found out by locked line to line test. Hence,

Copyright (c) 2013 IEEE. Personal use is permitted. For any other purposes, permission must be obtained from the IEEE by emailing pubs-permissions@ieee.org.

This article has been accepted for publication in a future issue of this journal, but has not been fully edited. Content may change prior to final publication.

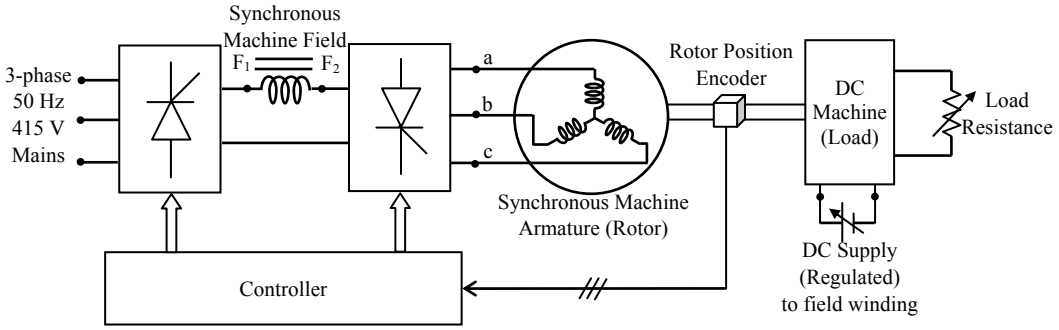

Fig. 11. Schematic block diagram of the experimental setup for the first method of validation on Machine #2.

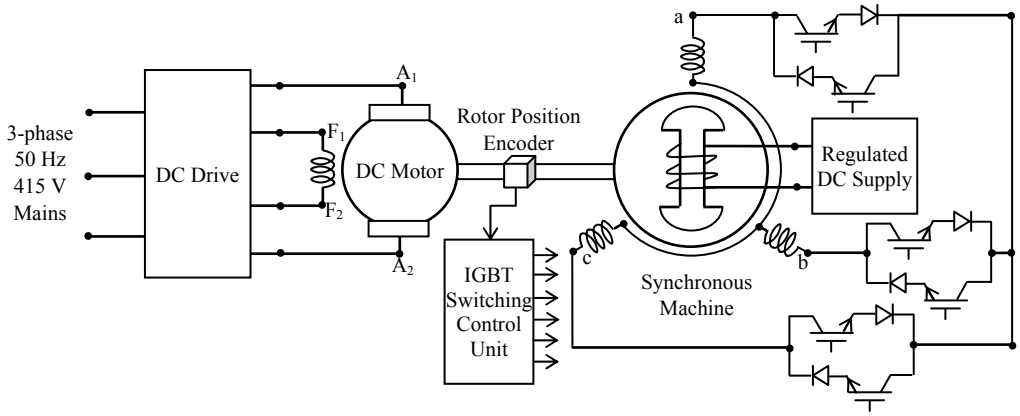

Fig. 13. Schematic block diagram of the experimental setup for the second method of validation on Machine #3.

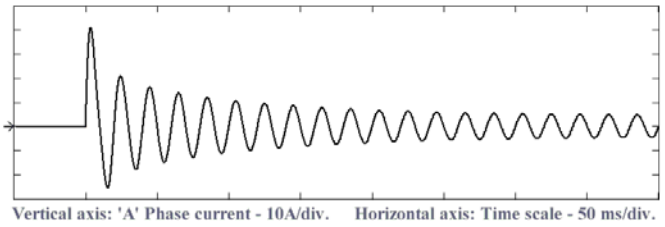

Fig. 14. Experimental waveform of the 'a' phase armature current of Machine #3, running at rated speed under a no-load condition, as per experimental setup of Fig. 13, when subjected to a three phase symmetrical short circuit at an instant when the field is in quadrature with the 'a' phase winding.

TABLE III
PARAMETERS OBTAINED FOR MACHINE #3 BY THE SECOND METHOD OF VALIDATION

Parameter	Value determined
r'_{fd}	0.158 Ω
L'_{lf}	12.3 mH
r'_{kd}	0.73 Ω
L'_{lkd}	4.58 mH
r'_{kq}	1.9 Ω
L'_{lkq}	10.66 mH

these two tests have been performed on Machine #3 to compare results for verification of the proposed methodology of determination of field and damper parameters. Fig. 13 shows the scheme of the experiment performed for the symmetrical short circuit test. An adjustable-speed DC drive at the front-end runs a DC motor, which acts as a prime-mover for the synchronous machine under test. The speed is maintained constant at 1500 r/min, which is the rated speed of Machine #3. The field current of Machine #3 is adjusted, so that the voltage at the armature terminals before short circuit at no-load condition is about 30% of the rated one. A three phase, four-quadrant controlled power electronic switch array involving insulated gate bipolar transistors (IGBT's) and diodes of large current (almost 40 times the rated current of Machine #3) and voltage ratings (almost 3 times the rated voltage of Machine #3) is used for creating the short circuit.

Initially the IGBTs are not gated and Machine #3 operates under no-load. The instant of the short circuit with respect to rotor position of Machine #3 can be precisely controlled by gating the IGBT's from the 'IGBT switching control unit', as the rotor position information is online made available to it (Fig. 13).

Fig. 14 shows the experimental current waveform of the 'a' phase of Machine #3 under three phase symmetrical short circuit, when the short circuit is initiated at an instant when the instantaneous the rotor (field) position is at quadrature with respect to the 'a' phase, so that the decaying asymmetrical DC component does not occur in the waveform [3, 5]. Similarly, the other phase current waveforms are also recorded. The symmetrical short circuit test is repeated with the condition when the rotor (field) position is aligned with the 'a' phase of the armature, by controlling the instant of short circuiting from the 'IGBT switching control unit' of Fig. 13. From these experimental waveforms, following the standard guidelines of [3, 5], using semilog graphs, the

Copyright (c) 2013 IEEE. Personal use is permitted. For any other purposes, permission must be obtained from the IEEE by emailing pubs-permissions@ieee.org.

This article has been accepted for publication in a future issue of this journal, but has not been fully edited. Content may change prior to final publication.

transient and subtransient reactances and time constants are determined. The locked line to line test [28] is next performed to experimentally determine the q-axis subtransient reactance. From the d-axis subtransient, transient reactances, q-axis subtransient reactance and the different d-axis and q-axis time constants thus obtained experimentally, the d-axis field and damper parameters and q-axis damper parameters are calculated. These values are entered in Table III and are found to be extremely close to the entries made in the third column of Table II, which are the values of the same machine parameters obtained by using the proposed methodology in this paper. Moroever, a difference of about 5% in the value of L'_{lkq} and 9% in the value of r'_{kq}, obtained from the proposed tests and the locked-line to line test, is an indication that the proposed methodology is fundamentally different from the existing locked line to line test.

V. Conclusions

In this paper, a standstill single phase AC voltage injection technique to any one armature phase of a three-phase wound field synchronous machine is presented, its mathematical justification is developed and analyzed with experimental findings to determine the d-axis and q-axis equivalent circuit damper and field parameters of the machine. The damper circuit in this testing methodology finds power frequency currents associated in them, which is close to mimicking sub-transient phenomena in synchronous machines and hence predicts the damper parameters accurately. This technique, to the best knowledge of the authors, has never been adopted previously in any research paper and is hence novel. It has been found and proved to be effective for small and medium sized wound-field synchronous machines. The methodology has been found to be simple and requires simpler, lesser sophisticated test infrastructure towards field and damper circuit parameter determination in a wound field synchronous machine of the referred power range, yet yields satisfactory results. The results obtained from the proposed methodology are validated successfully through experiments against similar results obtained from existing testing techniques/methodologies reported in the literature, on more than one synchronous machine of small and medium ratings.

VI. Appendix

The ratings of the 3-phase wound field synchronous machines are:

Machine #1: 3-phase, 208V, 60 Hz, 1800 r/min, 120VA, 0.33 A, rated field voltage 120V DC.

Machine #2: 3-phase, 400V, 50 Hz, 1500 r/min, 1.5 kVA, 2.2 A, rated field voltage 85V DC.

Machine #3: 3-phase, 380V, 50 Hz, 1500 r/min, 5 kVA, 7.6 A, rated field voltage 110V DC.

VII. References

[1] R. H. Park, "Two-Reaction theory of synchronous machines – generalized method of analysis – Part I," *AIEE Trans.*, vol. 48, pp. 716-728, 1929.

[2] R. H. Park, "Two-Reaction theory of synchronous machines – generalized method of analysis – Part II," *AIEE Trans.*, vol. 52, pp. 352-355, 1929.

[3] P. Kundur, *Power System Stability and Control*, vol. I. New York: McGraw-Hill, 1994.

[4] I. M. Canay, "Determination of model parameters of machines from the reactance operators $x_d(p)$ and $x_q(p)$ (Evaluation for standstill frequency response tests)," *IEEE Trans. Energy Conversion*, vol. 8, no. 3, pp. 272-279, 1993.

[5] *IEEE Guide: Test Procedures for Synchronous Machines Part I – Acceptance and Performance Testing, Part II – Test Procedures and Parameter Determination for Dynamic Analysis*, IEEE Standard 115-2009.

[6] *IEEE Guide: Synchronous Generator Modeling Practices and Applications in Power System Stability Analyses*, IEEE Standard 1110-2002.

[7] *ANSI/NEMA Guide for Motors and Generators*, *Rev. 1*, ANSI/NEMA MG1, 2006.

[8] J. Huang, K. A. Corzine, and M. Belkhayat, "Generation of Multisinusoidal Test Signals for the Identification of Synchronous-Machine Parameters by Using a Voltage-Source Inverter," *IEEE Trans. on Industrial Electronics*, vol. 57, issue 1, pp. 430 - 439, 2010.

[9] B. K. Bose, *Modern Power Electronics and AC drives*, USA: Pearson Education, 2002.

[10] R. S. Colby, M. D. Otto, and J. T. Boys, "Analysis of LCI synchronous motor drives with finite DC link inductance," *IEE Proc-B.*, vol. 140, no. 6, pp. 379-386, November 1993.

[11] A. K. Jain and V. T. Ranganathan, "Modeling and Field Oriented Control of Salient Pole Wound Field Synchronous Machine in Stator Flux Coordinates," *IEEE Transactions on Industrial Electronics*, vol. 5, issue 6, pp. 960 - 970, 2011.

[12] P. L. Dandeno, R. L. Hauth, and R. P. Shulz, "Effects of synchronous machine modeling in large scale system studies," *IEEE Trans. Power App. Syst.*, vol. PAS-92, pp.574-582, Mar. /Apr. 1973.

[13] S. H. Minnich, R. P. Schulz, D. H. Baker, R. G. Farmer, D. K. Sharma, and J. H. Fish, "Saturation functions for synchronous generators from finite elements," *IEEE Trans. Energy Conversion*, vol. EC-2, pp. 680–692, Dec. 1987.

[14] R. P. Schulz, C. J. Goering, R. G. Farmer, S. M. Bennett, and D. A. Selin, "Benefit assessment of finite-element based generator saturation model," *IEEE Trans. Power Syst.*, vol. PWRS-2, pp. 1027–1033, Nov. 1987.

[15] F. S. Sellschopp and M. A. Arjona, "DC decay test for estimating d-axis synchronous machine parameters: a two-transfer function approach," in proc. of *IEE Elect. Power Appl.*, vol. 153, no.1, Jan. 2006.

[16] P. J. Turner, A. B. J. Reece, and D. C. Macdonald, "The D.C. decay test for determining synchronous machine parameters: measurements and simulation," *IEEE Trans. Energy Convers*., pp.616–623, 1989.

[17] A. Tumageanian and A. Keyhani, "Identification of synchronous machine linear parameters from standstill step voltage input data," *IEEE Trans. Energy Convers*., pp. 232–240, 1995.

[18] A. Tumageanian, A. Keyhani, S. I. Moon, and T. I. Leksan, "Maximum likelihood estimation of synchronous machine parameters from flux decay data," *IEEE Trans. Ind. Appl*., pp. 433–439, 1994.

[19] Y. Jin, and A. M. El-Serafi, "A three transfer functions approach for the standstill frequency response test of synchronous machines," *IEEE Trans. Energy Convers*., pp. 740–749, 1993.

[20] *IEEE* Standard: 'Standard procedures for obtaining synchronous machines parameters by standstill frequency response testing' IEEE Standard 115A-1995

[21] P. C. Krause, O. Wasynczuk, and S. Sudhoff, *Analysis of Electric machinery and Drive Systems*, Wiley-IEEE Press, 2002.

[22] M. G. Say, *The Performance and Design of Alternating Current Machines*, London: Pitman Publishing, 1968.

[23] A. M. El-Serafi and J. Wu, "A New Method for Determining the Leakage Reactance of Synchronous Machines," *IEEE Trans. Energy Conversion*, vol. 6, no. 1, pp. 120-125, 1991.

[24] N. C. Kar and A. M. El-Serafi, "The Experimental Methods for measuring the q-axis saturation characteristics of synchronous machines," in *Proc. 2004 IEEE Canadian Elec. and Comp. Engg. Conf.*, pp. 425-428.

Copyright (c) 2013 IEEE. Personal use is permitted. For any other purposes, permission must be obtained from the IEEE by emailing pubs-permissions@ieee.org.

This article has been accepted for publication in a future issue of this journal, but has not been fully edited. Content may change prior to final publication.

[25] N. C. Kar and A. M. El-Serafi, "Measurement of the saturation characteristics in the quadrature axis of the synchronous machines," *IEEE Trans Energy Conversion.*, vol. 21, no. 3, pp. 690-698, 2006.
[26] S. SenGupta, K. Mukherjee, T. K. Bhattacharya and A. K. Chattopadhyay, "Performance of an SCR-inverter-based commutatorless series motor with load commutation and unaided startup capability," *IEEE Trans Industry Applications.*, vol. 36, no. 4, pp. 1151-1157, July/August 2000.
[27] B. Mueller, T. Spinanger and D. Wallstein, "Static variable frequency starting and drive system for large synchronous motors," in *Proc. 1979 IEEE-IAS Annual Meeting*, pp. 428-438.
[28] I. Boldea, *The Electric Generators Handbook- Synchronous Generators*, Boca Raton, USA: CRC Press, Taylor & Francis Group, 2006.

VIII. BIOGRAPHIES

Kaushik Mukherjee (M'03) was born in 1970. He received the B.E. degree from the Department of Electrical Engineering, Jadavpur University, Calcutta, India, in 1993, the M.E. degree from the Department of Electrical Engineering, Bengal Engineering College, Howrah, India, in 1998, and the Ph.D. degree from the Department of Electrical Engineering, Indian Institute of Technology, Kharagpur, India, in 2003. Since 1993, he has spent almost two and a half years in the industry. In 2002, he joined the Department of Electrical Engineering, Jadavpur University, India as a Lecturer. From 2006 onwards, he is an Assistant Professor in the Department of Electrical Engineering, Bengal Engineering and Science University, Howrah, India. Dr. Mukherjee is presently a Visiting Professor at the Centre for Hybrid Automotive Research & Green Energy, University of Windsor, Canada. His research interests include electrical machine drives and power electronics applications in general.

K. Lakshmi Varaha Iyer received the B.Tech. degree in Electronics and Communication Engineering from SASTRA University, India, in the year 2009 and the M.A.Sc. degree in Electrical and Computer Engineering from University of Windsor, Canada in the year 2011. He is currently a Research Associate at the Centre for Hybrid Automotive Research and Green Energy, University of Windsor, Canada. His research presently focuses on design & control of electric machines and condition monitoring for renewable energy applications.

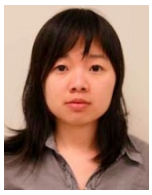

Xiaomin Lu received her Bachelor in Engineering from Sun-Yet Sen University, China in July, 2010. She is currently working towards her M.A.Sc degree at University of Windsor, Ontario, Canada. Her research areas include modeling and analysis of permanent magnet synchronous machines & drives and condition monitoring for electric vehicle drive-train system and power system applications.

Narayan C. Kar received the B.Sc. degree in Electrical Engineering from Bangladesh University of Engineering and Technology, Dhaka, Bangladesh, in 1992 and the M.Sc. and Ph.D. degrees in electrical engineering from Kitami Institute of Technology, Hokkaido, Japan, in 1997 and 2000, respectively. He is an associate professor in the Electrical and Computer Engineering Department at the University of Windsor, Canada where he holds the Canada Research Chair position in hybrid drivetrain systems. His research presently focuses on the analysis, design and control of permanent magnet synchronous, induction and switched reluctance machines for hybrid electric vehicle and wind power applications, testing and performance analysis of batteries and development of optimization techniques for hybrid energy management system. He is a Senior Member of the IEEE.

Copyright (c) 2013 IEEE. Personal use is permitted. For any other purposes, permission must be obtained from the IEEE by emailing pubs-permissions@ieee.org.